Catalysis Letters Vol. 106, Nos. 3–4, February 2006 (© 2006)
DOI: 10.1007/s10562-005-9617-1

Studies on preparation, characterization and ammoxidation functionality of zirconium phosphate-supported V_2O_5 catalysts★

Ch. Srilakshmi, K. Ramesh, P. Nagaraju, N. Lingaiah, and P. S. Sai Prasad*

Indian Institute of Chemical Technology, Hyderabad 500 007, India

Received 30 June 2005; accepted 18 October 2005

Zirconium pyrophosphate (ZrP_2O_7) was synthesized from zirconyl chloride and phosphoric acid. A series of ZrP_2O_7-supported V_2O_5 catalysts, with the oxide loading ranging from 2 to 8 wt.%, was prepared by wet impregnation method. These catalysts were characterized by various techniques like X-ray diffraction, BET surface area, pore size distribution, FT-IR spectroscopy, acidity measurements and X-ray photoelectron spectroscopy. Their catalytic functionality was evaluated in the ammoxidation of 2-methyl pyrazine (MP) to 2-cyano pyrazine (CP). The V_2O_5/ZrP_2O_7 catalysts are found to be highly active and selective. FT-IR profiles of used catalysts indicate the interaction of ammonia with vanadia. The physico-chemical properties of the catalysts are correlated with their activity and nitrile selectivity.

KEY WORDS: vanadia catalysts; zirconium pyrophosphate; ammoxidation of 2-methyl pyrazine; vanadium ammonium complex.

1. Introduction

In the recent past, metal phosphates have attracted considerable attention as solid acid catalysts [1–5]. The activity of these materials is attributed to the Bronsted acidity of hydroxyl groups and the Lewis acidity of the metal centre. In particular, zirconium phosphates have been used in catalytic reactions such as dehydration of alcohols and isomerization of olefins [6–10]. Owing to their textural and acid properties these are also used as supports for other catalytically active inorganic species [11].

Supported vanadium oxides form an industrially important class of active catalysts. They have been studied quite extensively because of their use in several processes [12–19]. Generally, bulk V_2O_5 cannot be used as a catalyst due to its poor thermal stability and mechanical strength and low active surface area. Therefore, vanadium oxide is normally supported on different carriers depending on the type of reaction to be catalysed. Various single oxides such as Al_2O_3, TiO_2, SiO_2 are commonly employed as supports for dispersing vanadium oxide. Metal oxide-supported vanadia catalysts particularly find application in the ammoxidation of aromatic hydrocarbons to their corresponding nitriles [20–22]. With respect to metal phosphate, vanadia supported on layered titanium phosphate has been used as a catalyst for the oxidation of *o*-xylene, showing reasonable partial oxidation property [5,23].

The ammoxidation of MP is a reaction of recent interest since the CP produced is further transformed to 2-amidopyrazine (popularly called as pyrazinamide, an anti-tubercular drug). It has been observed that the most frequently used commercial vanadia-based catalysts, for example V/Sb and V/Ti, are highly active. The main disadvantages of these catalysts are that they operate at high reaction temperatures and produce considerable amounts of by-products. At a time when environmental protection is given high priority in chemical synthesis, it is detrimental to continue with the low selective catalytic processes. In this context, we have recently observed that bulk metal phosphates offer very high nitrile selectivity during the ammoxidation of MP [24]. But their activity is found to be low. Besides, there are no reports in the literature on ammoxidation of MP to CP catalysed by vanadium oxide supported on metal phosphate catalysts. Though, there have been a good number of applications for zirconium pyrophosphate as catalyst, its use as support material is also less explored. Therefore, it is interesting to study the performance of zirconium phosphate-supported vanadia catalysts in the synthesis of CP from MP. The present study has been undertaken to understand the catalytic functionality of V_2O_5/ZrP_2O_7 catalysts in enhancing the conversion and product selectivity. The catalysts have been thoroughly characterized and the physico-chemical properties thus obtained are correlated with the activity and selectivity of the catalyst measured in the transformation of MP.

2. Experimental

2.1. Catalyst preparation

In the present study, zirconium pyrophosphate was directly synthesized by reacting zirconium oxychloride

★IICT Communication No. 050602

* To whom correspondence should be addressed.
E-mail: saiprasad@iict.res.in

($ZrOCl_2$) and *ortho*-phosphoric acid (H_3PO_4). The required stoichiometric amount of $ZrOCl_2{\cdot}8H_2O$ (50 g) was dissolved in 100 mL of double distilled water. After complete dissolution, H_3PO_4 (85%) was added dropwise. The white precipitate thus obtained was washed thoroughly several times with distilled water until the chloride ions in the filtrate were completely removed. This was ensured by titrating the filtrate, after each washing, with silver nitrate solution and the disappearance of white precipitate suggested its absence. The filtered precipitate was dried at 393 K for 12 h. The dry cake was then calcined at 773 K for 5 h. V_2O_5/ZrP_2O_7 catalysts with vanadia content ranging from 2.0 to 8 wt.% were prepared by impregnation of the support with varying quantities of an oxalic acid solution (typically 2.3 g of oxalic acid in 5 mL water) containing ammonium metavanadate. The catalysts were subsequently dried at 383 K for 16 h and calcined at 723 K for 5 h.

2.2. Catalyst characterization

X-ray diffraction (XRD) patterns of the catalysts were obtained on a Siemens D-5000 diffractometer, using CuK_α radiation. BET surface area was determined on a Micromeritics (Tristar 3000) instrument with nitrogen physisorption at 77 K, taking 0.169 nm^2 as the cross sectional area of dinitrogen. Pore size distribution measurements were also conducted on the same instrument. Prior to surface area and pore size distribution measurements the catalysts were pretreated in helium at 473 K for 90 min.

FT-IR spectra were recorded on a Nicolet 740 spectrometer using the KBr disc method. X-ray photoelectron spectra were recorded on KRATOS AXIS 165 equipped with a dual anode (Mg and Al) apparatus using the MgK_α anode and hemispherical analyzer, connected to a five channel detector. The background pressure during data acquisition was kept below 10^{-10} torr. Binding energy correction was performed by using the 182.3 eV as reference for V_2O_5/ZrP_2O_7 catalysts. Spectra were de-convoluted using Sun Solaris-based curve resolver. The location and the full width at half maximum (FWHM) value for the species was first determined using the spectrum of the pure sample. The location and FWHM of products, which were not obtained as pure species, were adjusted until the best fit was obtained. Symmetric Gaussian shapes were used in all cases. Binding energies for identical samples were, in general, reproducible within ±0.1 eV.

The acidic strength of the solid samples was measured by the potentiometric titration method. A known mass of solid, suspended in acetonitrile, was stirred for 3 h and then the suspension was titrated with a solution of 0.05 N *n*-butylamine in acetonitrile, at a flow rate of 0.05 mL/min. The variation in the electrode potential was measured in a microprocessor-based autotitrator (Schott, Germany). The technique enables determination of acidic strength and also the total number of acid sites. In order to interpret the results, the initial electrode potential (E_i) is taken as the maximum acidic strength of the surface sites [25]. The acidic strength of surface sites is assigned according to the following ranges [26]: very strong site, $E_i > 100$ mV: strong site, $0 < E_i < 100$ mV; weak site $-100 < E_i < 0$ mV and very weak site $E_i < -100$ mV.

2.3. Catalyst evaluation

The ammoxidation reaction was carried out in a vertical fixed bed, continuous down flow micro-reactor made of quartz, under atmospheric pressure. In a typical experiment, about 3 g of the catalyst (sieved to 18/25 BSS mesh, to avoid mass transfer limitations), diluted with an equal amount of quartz grains, was packed between two layers of quartz wool in the reactor. The upper portion of the reactor was filled with quartz beads that served both as a pre-heater and a mixer for the reactants. An aqueous mixture of MP (MP:Water = 1:2.5, v/v) was fed into the reactor by means of a microprocessor-controlled metering pump (B. Braun, Germany). The molar ratio of the feed was kept at MP:water:ammonia:air = 1:13:7:40, maintaining a W/F_{liquid} ratio = 2.0 g cm^{-3} h. The reaction temperature was monitored by a thermocouple with its tip located in the catalyst bed and connected to a PID-type temperature indicator-controller. The reaction occurred in the flow integral mode. The reaction was carried out at various temperatures ranging from 633 to 693 K. The liquid product collected, after the catalyst had attained a steady state, was analysed by gas chromatography. From the analysis of non-condensable exit gas mixture, it was ensured that the quantity of any organic species was negligible. The steady state was attained after 1 h and the activity remained constant for 10 h. The zirconium phosphate support was also evaluated for the sake of comparison. The conversion was calculated based on the disappearance of MP, The selectivity to CP was calculated as follows:

$$\%\text{Selectivity} = \frac{\text{Moles of CP formed}}{\text{Moles of MP converted}} \times 100$$

3. Results and discussion

3.1. The structure of vanadia on the support

XRD patterns of pure zirconium pyrophosphate and zirconium pyrophosphate-supported vanadium oxide catalysts, with vanadia loading ranging from 2 to 8 wt.%, are shown in figure 1. It can be seen from the figure that all the samples showed XRD peaks due to zirconium pyrophosphate with major peaks at $d = 4.12$ Å, 3.69 Å and 4.47 Å. The d values obtained in

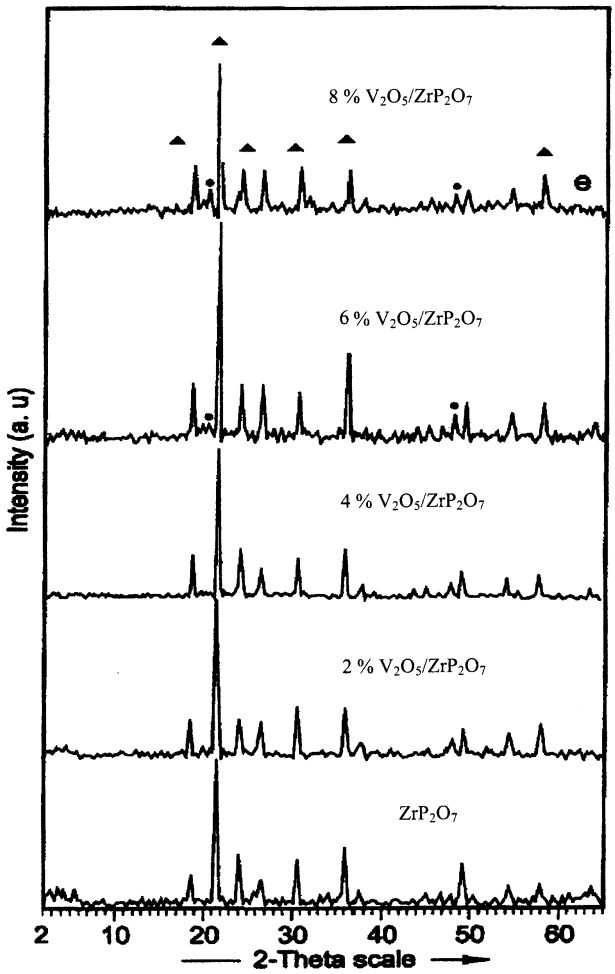

Figure 1. Powder XRD patterns of calcined V_2O_5 supported on zirconium phosphate catalysts as a function of V_2O_5 loading.

the present work closely match with those given in JCPDS file No-12-1399 pertaining to zirconium pyrophosphate. This result confirms the formation of zirconium pyrophosphate. For samples less than 6 wt.% V_2O_5 no XRD peaks corresponding to vanadium oxide are observed indicating that the oxide is present in a highly dispersed state on zirconium pyrophosphate. However, the presence of vanadia crystallites having size less than 4 nm, which is below the detection capacity of powder XRD technique, cannot be ruled out. The XRD peaks corresponding to V_2O_5 appearing at $2\theta = 20.26°$ can be seen only from 6 wt.% V_2O_5/ZrP_2O_7 sample, and its intensity is found to increase with increase in vanadia loading. This means that the active component–support interaction is weak at higher vanadium concentrations where vanadium starts forming vanadium oxide crystals rather than spreading over the surface. From figure 1 it can also be deduced that there is no formation of any compound due to the interaction between V_2O_5 and ZrP_2O_7.

The results of BET surface area, pore volume and average pore diameter of various V_2O_5/ZrP_2O_7 catalysts, measured by nitrogen physisorption, are also presented in table 1. The specific surface area of ZrP_2O_7 support is found to be 10.2 $m^2\ g^{-1}$ and it decreased as the vanadia content increases. A continuous decrease of surface area and pore volume with increasing vanadia loading might be due to progressive blocking of pores of the support, particularly at higher loading by crystalline vanadium oxide, as evidenced by XRD. The corresponding pore size distribution curves (not shown here) showed that this decrease is accompanied by progressive disappearance of the relatively narrow pores of the support and simultaneous creation of wider pores. This result is evidenced by the shift in the average pore diameter to higher values.

The FT-IR spectra of ZrP_2O_7 and various V_2O_5/ZrP_2O_7 catalysts are shown in figure 2. The infrared spectrum of the support shows strong absorption bands at 3400–2400, 1600, 1114, 976, 744 and 548 cm^{-1}. The bands in the region 3400–2400 cm^{-1} are due to surface OH groups. The band at 1600 cm^{-1} is due to bending vibrational mode of OH group. The band at 1115 cm^{-1} is due to symmetric stretching modes of PO_2 group from pyrophosphate, while the bands at 976 and 744 cm^{-1} are due to asymmetric and symmetric stretching modes of P–O–P bonds, respectively, in the chains [27,28] and the band at 548 cm^{-1} is due to bending mode of O–P–O bond. The spectra of catalysts with V_2O_5 content of 6 wt.% and above show a small band at 638 cm^{-1}. This band is due to V–O–V deformation mode. Thus, in samples containing less than 6 wt.% active component, vanadia is stabilized by interaction with the support surface and is present in a form not detectable as bulk V_2O_5. These findings are in good agreement with the XRD results. According to Nakagawa *et al.* [29] vanadium oxide on the support surface is present as an amorphous V_2O_5 at lower vanadia loading and

Table 1
Physico-chemical properties of the support and ZrP_2O_7 supported-V_2O_5 catalysts

Catalyst (wt.% of V_2O_5)	Surface area ($m^2\ g^{-1}$)	Pore volume ($cm^3_{(STP)}\ g^{-1}$)	Average pore diameter (nm)	Acidic strength E (mV)
ZrP_2O_7	10.2	0.0254	5.16	642
2	6.8	0.0228	11.07	298
4	4.7	0.0219	9.66	320
6	4.0	0.0187	10.6	408
8	1.2	0.0101	20.6	438

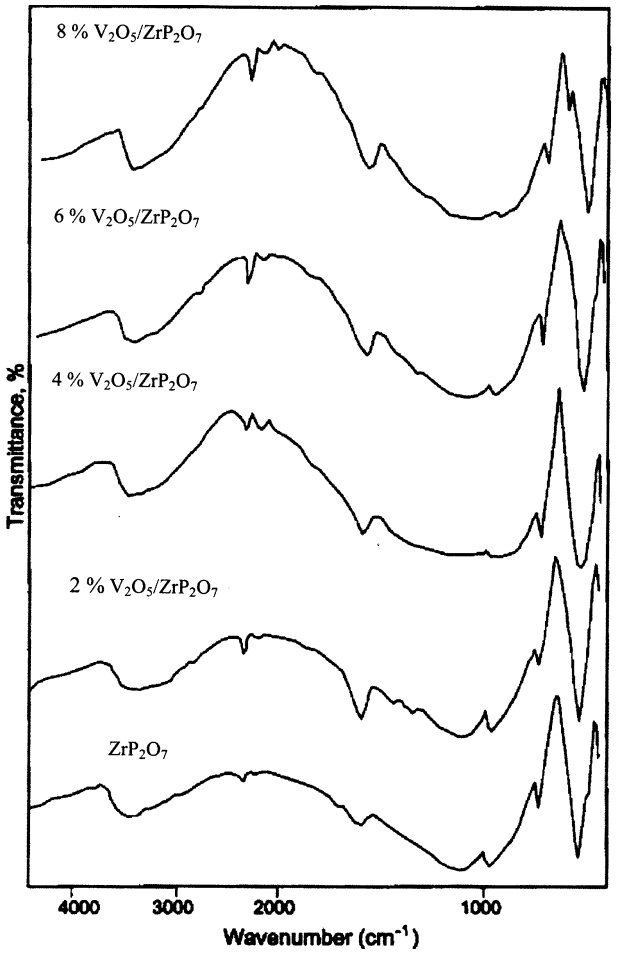

Figure 2. The FT-IR spectra of the fresh V_2O_5 supported on zirconium phosphate catalysts.

amorphous and crystalline V_2O_5 at higher vanadia contents. Several studies using IR technique have also supported these observations.

3.2. Change in acidic properties with vanadia loading

In the present investigation the acidity measurements have been carried out using *n*-butylamine. The profiles are shown in figure 3. The acidic strength values, are given in table 1. From the values given in the table it is clear that the support possesses very strong surface acidic sites. This type of very strong acidity of the ZrP_2O_7 is also observed by Benvenuti *et al.* [30]. With the deposition of 2 wt.% V_2O_5, the acidic strength is found to decrease considerably. From this observation it may be inferred that the very strong surface acidic sites of ZrP_2O_7 are suppressed and only moderately strong surface acidic sites are generated due to patchy dispersion of V_2O_5 on the surface of the support. With increase in V_2O_5 loading from 2 to 8 wt.% the acid strength values increased further, suggesting that the deposition of vanadium oxide on ZrP_2O_7 helps increase the strength of the surface acidic sites moderately. It is observed that there is no significant change in the

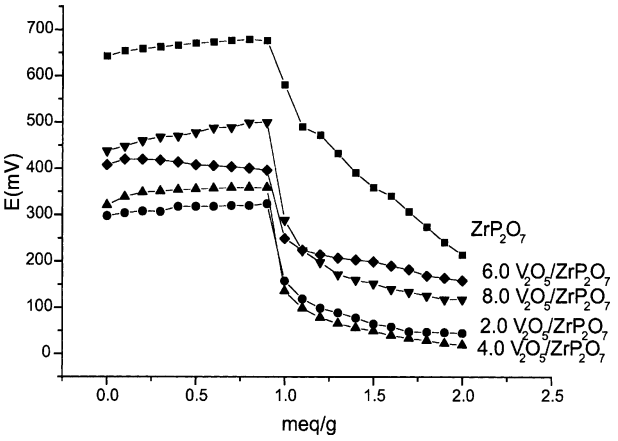

Figure 3. Potentiometric titration profiles of various V_2O_5/ZrP_2O_7 catalysts.

number of acid sites, as expressed by meq/g catalyst, as all curves have shown nearly the same (1.1 meq/g) value at the plateau regions. This may be the manifestation of low specific surface area of the catalysts.

3.3. Vanadia dispersion by XPS studies

XPS studies have been employed for the surface characterization of V_2O_5/ZrP_2O_7 catalysts. The V2p XPS spectra of various catalysts with different V_2O_5 loadings, are shown in figure 4. In the XPS spectra the major peaks can be attributed to $V2p_{3/2}$, $V2p_{1/2}$. The $V2P_{3/2}$ peak appears at around 517 eV and the

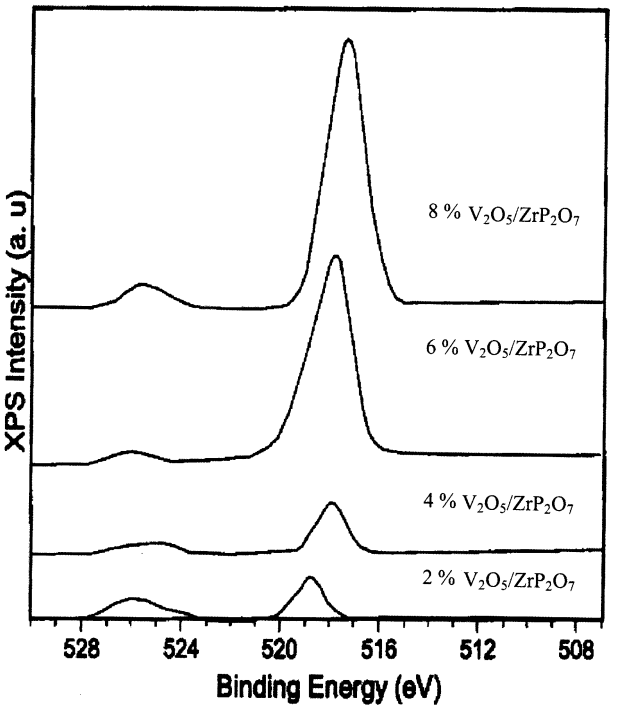

Figure 4. $V2p_{3/2}$ XPS spectra of various V_2O_5 supported on zirconium phosphate catalysts.

Table 2
Results of X-ray photoelectron spectroscopy of various V_2O_5/ZrP_2O_7 catalysts

V_2O_5 loading (w/w)	Position and FWHM of $V2p_{3/2}$	Position and FWHM of $Zr3d_{5/2}$	XPS intensity ratio
2	518.7 (1.24)	183.8 (1.55)	6.98
4	517.9 (1.39)	183.7 (1.48)	9.56
6	516.8 (1.81)	183.5 (1.64)	5.24
8	517.4 (1.87)	183.6 (1.54)	2.21

corresponding spin-orbit doublet, $2p_{1/2}$ appears at about 525 eV. The reported binding energy values of present series of catalysts (table 2) fit well with that of V species with 5+ oxidation state. No indication of ions with lower oxidation state of V is observed in all the calcined samples. This can also be evidenced from the FWHM values, which are present in between 1.24 and 1.87 (table 2). The intensity of the vanadium peaks increased with the increase in vanadium loading.

Figure 5 shows the Zr 3d XPS spectra of the catalysts. In all the samples Zr $3d_{5/2}$ binding energies are found to be around 183 eV which fits well with the (4^+) oxidation state of Zr in zirconium phosphate, as reported by Moulder *et al.* [31].

The values of the ($V2p_{3/2}$ to Zr $3d_{5/2}$) XPS intensity ratio (table 3) increased with the increase in V_2O_5 loading up to 4 wt.% catalyst and then showed deviation from linearity indicating formation of vanadium oxide crystals at and above 6 wt.% catalyst. Thus V2p/Zr3d ratio indirectly gives the information about the dispersion of vanadium oxide on zirconium pyrophosphate support. The results suggest that at low V_2O_5 loadings the dispersion of V_2O_5 is high and at higher V_2O_5 loadings crystalline vanadium oxide is formed.

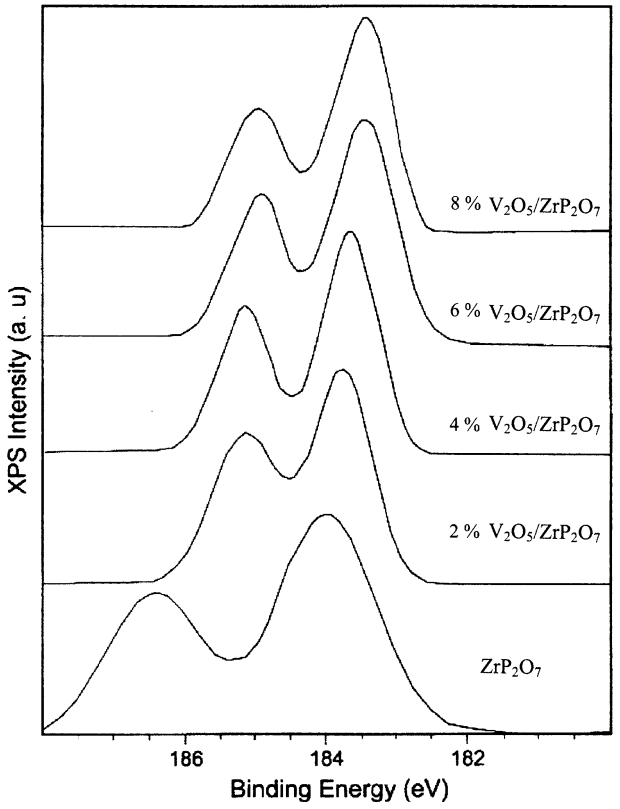

Figure 5. $Zr3d_{5/2}$ XPS spectra of various V_2O_5 supported on zirconium phosphate catalysts.

3.4. *The ammoxidation activity as a function of vanadia loading*

Table 3 displays the variation of activity of the catalysts with vanadia loading during the ammoxidation of MP to CP at different reaction temperatures, 633–693 K. At a typical temperature of 693 K the support gave only 18% conversion of MP. At the same reaction temperature, the conversion recorded a very high value with the incorporation of vanadia on the surface of the support. This is an important observation. Further, it is found to increase with increase in vanadia loading up to 4 wt.% (from 76% at 2 wt.% loading and 95% at 4 wt.%). The MP conversion has slightly decreased at higher loading. As already reported earlier, the formation of vanadium oxide crystallites is observed by XRD studies in 6 and 8 wt.% catalysts. BET surface area is also found to decrease considerably at this loading. However, the conversion increased with increasing reaction temperature at all loadings, apparently due to kinetic effect. These results, in combination with those of characterization, indicate that the dispersed vanadia sites are specifically active in the transformation of MP. Table 3 also provides the data on variation in the XPS intensity ratio with vanadium loading. A good proportionality between the XPS intensity ratio and MP conversion can be observed. Many authors have also used the XPS intensity ratio to predict the trend in vanadia dispersion on the support, particularly when V_2O_5 is supported on metal oxides. In a recent work [32] it has also been proved that similar trend in dispersion behaviour can be obtained by both gas adsorption and XPS intensity ratio techniques. Though the XPS intensity ratio may not provide an absolute value for dispersion, it can be safely considered to understand the general dispersion pattern of vanadia on the support surface. Thus, in the present case, the ammoxidation activity is found to be directly proportional to vanadia dispersion, as calculated by the XPS intensity ratio. Chary *et al.* [33] have also reported that the catalytic active sites of vanadia (dispersed on aluminium phosphate), responsible for

Table 3
Variation of XPS intensity ratio and the conversion of MP with vanadia loading on ZrP_2O_7-supported catalysts

V_2O_5 loading (wt.%)	XPS intensity ratio	Conversion of methylpyrazine (%) at different reaction temperatures			
		633 K	653 K	673 K	693 K
2	6.98	55	61	73	76
4	9.56	88	91	93	95
6	5.24	76	88	90	92
8	2.21	74	83	85	88

the ammoxidation of 3-picoline to nicotinonitrile, are located on a patchy monolayer phase.

The influence of acidity on the ammoxidation activity is also studied by several researchers. The general conclusion is that the total acidity/acidic strength alone does not seem to be responsible for the activity in the case of supported V_2O_5 catalysts, as linear correlations could not be obtained between the two. A similar observation is also recorded in the present investigation also. It is also the redox property that seems to be important. Courtine and Bordes [34] are under the impression that the improvement in catalytic performance is due to the modification of the redox as well as acid–base properties of the monolayer (compared to crystalline vanadia), as much lower acidity is exhibited by the monolayer.

3.5. *The role of strength of the acid site on nitrile selectivity*

Figure 6 shows the dependence of the selectivity to CP as a function of vanadia loading at different reaction temperatures, in the range of 633–693 K. The selectivity to CP is found to increase with vanadia content up to 6 wt.% and reached a maximum value of 87.7% at 633 K and decreased slightly with further addition of V_2O_5. Two important observations can be made at this juncture. The first observation is that the CP selectivity is found to be independent of vanadia loading. Secondly, it is also strictly not dependent on the acidic strength. It is interesting to note here that the acidic strength decreased initially (when compared to that of the support) but gradually increased with increase in vanadia loading. Very high acid strength of the support resulting in low CP selectivity (35% at 633 K) implies that an optimum acidic strength may be necessary for the favourable formation CP. The high values of CP selectivity obtained on V_2O_5/ZrP_2O_7 (compared to that on the support) might be the manifestation of reduction in surface acidic strength by progressive replacement of the strong acid sites of the support with moderately acidic sites of V_2O_5. It could be predicted that whereas moderately strong acid sites help in the chemisorption of MP, the very strong acid sites promote further dealkylation of the adsorbed reactant leading to pyrazine formation. However, this proposition requires additional experimental evidence since due consideration should also be given to the fact that at conversions more than 60% the selectivity decreases due to after oxidation of the nitrile formed.

Figure 7 displays the dependence of selectivity to pyrazine on vanadia loading at different reaction temperatures, 633–693 K. The selectivity to pyrazine is found to be 65% on the bare support. However, it

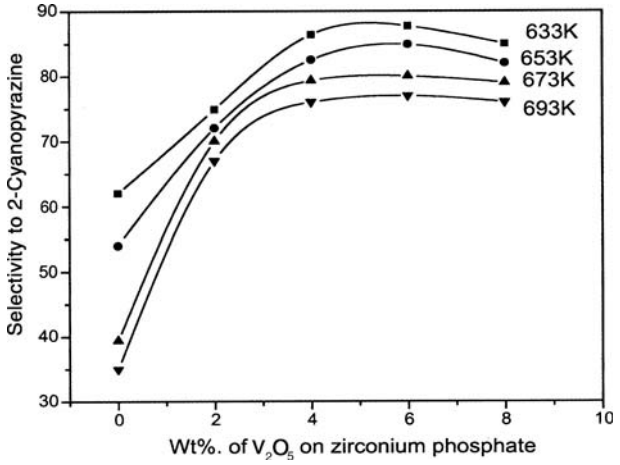

Figure 6. Dependence of selectivity to cyanopyrazine as a function of V_2O_5 loading on zirconium phosphate at different temperatures.

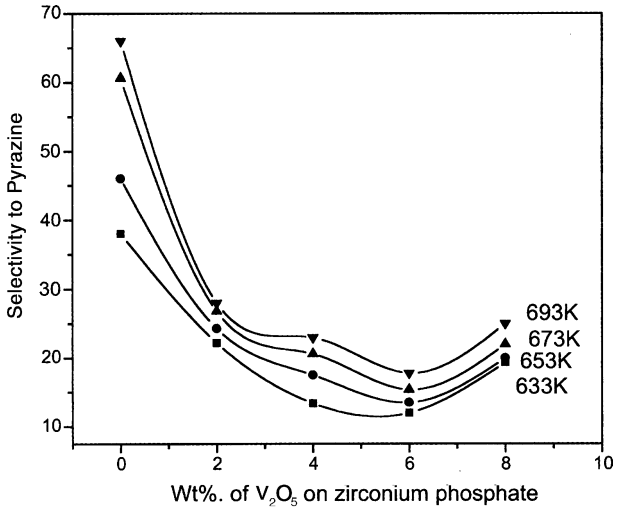

Figure 7. Dependence of selectivity to pyrazine as a function of V_2O_5 loading on zirconium phosphate at different temperatures.

decreased with increasing vanadia loading from 2 to 6 wt.% reaching a value of 17.8% (at 693 K). This could be due to decrease in acid strength. At higher loadings of vanadia i.e., at 8 wt.% the selectivity to pyrazine increased slightly again and reached a value of 25%.

3.6. Formation of ammonium compound during the reaction

Figure 8 shows the IR spectra of used ZrP_2O_7 and V_2O_5/ZrP_2O_7 catalysts. The spectra of used catalysts showed the bands at 1402, 1109, 976, 743 and 546 cm^{-1}. The new band at 1402 cm^{-1} is due to ammonium ion. The intensity of the band increased with vanadia loading. This could be due to the progressive formation of an ammonium compound in the used catalysts. At low vanadia loadings the dispersed species are highly susceptible to the formation of an ammonium complex. At higher vanadia loading the presence of crystalline vanadia controls the formation of the ammonium compound.

This observation is remarkable since molecular ammonia is being attached to the surface as ammonium ion during the ammoxidation reaction. This result also suggests that surface ammonium ions participated during the ammoxidation reaction. The formation of NH_4VO_3 phase, during the ammoxidation reaction, is reported by Narayana *et al.* [35]. Literature also reveals that pure V_2O_5 develops a V_3O_5 phase and an $NH_4V_4O_{10}$ phase due to interaction of NH_3 with vanadia. Martin *et al.* [36] have clearly brought out the involvement of surface ammonium ion in the ammoxidation mechanism, particularly to interpret the results to nitrile selectivity. It may be construed that the moderate acidic strength of the catalysts helps in fixing ammonia to the V surface forming an ammonium compound between them. This new species, which need to be identified, enhances the nitrile selectivity.

It is prudent at this juncture, to compare the activity and selectivity of the zirconium phosphate-supported vanadia catalysts, in the ammoxidation of MP, with those reported in the literature. As such, there is no report on the application of vanadia supported-metal phosphates for the ammoxidation reaction. However, a comparison of the results obtained on vanadia supported on other metal phosphates in our laboratory and the catalysts reported by Forni [37], is provided in table 4. It can be observed that the present class of catalysts is more active and selective than those already reported.

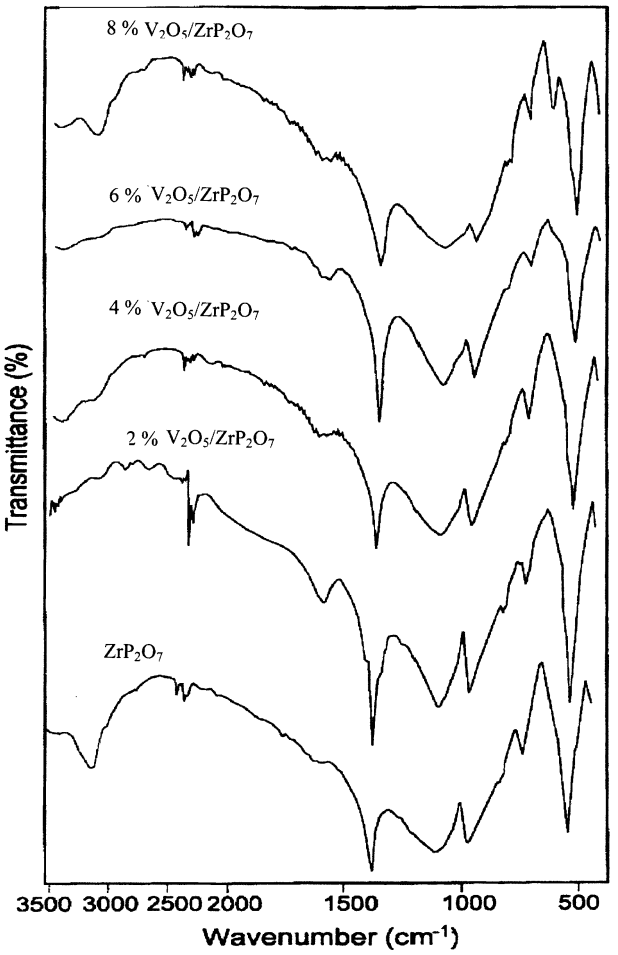

Figure 8. The FT-IR spectra of the used V_2O_5 supported on zirconium phosphate catalysts.

4. Conclusions

Bulk zirconium pyrophosphate as well as zirconium pyrophosphate-supported vanadia were found to be

Table 4
A comparison of the activity and selectivity of the present catalysts with those reported in the literature

Type of catalyst	Temperature (K)	Conversion of 2-methylpyrazine	Selectivity to 2-CP	Selectivity to pyrazine
V_2O_5/ZrP_2O_7	673	90	80	15
$V_2O_5/NbOPO_4$	673	69	48	46
$V_2O_5/AlPO_4$	673	42	52	47
V-CrO_X/Al_2O_3[a]	673	53	22	58
α-$VOPO_4$[b]	673	40	68	30
β-$VOPO_4$[b]	673	29	60	37

[a]Reference No. [34]
[b]Reference No. [22]

active catalysts during ammoxidation of MP. The bulk catalyst shows high selectivity towards pyrazine, which is due to dealkylation catalysed by sites of high acidic strength. Addition of vanadia plays a decisive role in decreasing acidic strength and increasing the activity and selectivity. FT-IR results of used catalysts show the presence of ammonium complex formation. This observation is remarkable since the NH_3 in the reactant stream indeed reacts with the surface during the ammoxidation, forming an ammonium compound which improves the nitrile selectivity.

Acknowledgements

CHSL and KR thank Council of scientific and industrial research (CSIR), New Delhi for awarding senior research fellowships. Thanks are due to Director, IICT, for allowing publishing these results.

References

[1] R.B. Borade, B. Zhang and A. Clearfield, Catal. Lett. 45 (1997) 233.
[2] M.C.C. Costa, R.A.W. Johnstone and D. Whittaker, J. Mol. Catal. A 129 (1998) 79.
[3] A. Johnstone, P. J. Middleton, R. C. Wasson, R.A.W. Johnstone, P.J.C. Pires, G.M.S.R.O. Rocha, in: *The Activation of Dioxygen and Homogeneous Catalytic Oxidation*, eds. D.H.R. Barton et al. (Plenum Press, New York, 1993), p. 45.
[4] M.C.C. Costa, L.F. Hodson, R.A.W. Johnstone, J. Liu and D. Wittaker, J. Mol. Catal. A 142 (1999) 349.
[5] I.C. Marcu, I. Sandulescu and J.M. Millet, J. Mol. Catal. A: Chem. 203 (2003) 241.
[6] A. Clearfield and T.S. Takur, J. Catal. 65 (1980) 185.
[7] A. La Ginestra, P. Patrono, M. L. Berardelli, P. Galli, M.A. Massucci, C. Ferragina and P. Ciambelli, *Proc. XIX Congr. Naz. Chim. Inorg, S. Margheria di Pula*, Cagliari, Italy, 1986, p. 439.
[8] K. Segawa, Y. Kurusu, Y. Nakajima and M. Kinoshita, J. Catal. 94 (1985) 491.
[9] A. La Ginestra, P. Partono, M.L. Berardelli, P. Galli, C. Ferragina and M.A. Massucci, J. Catal. 103 (1987) 346.
[10] G. Ramis, P.F. Rossi, G. Busca, V. Lorenzelli, A. La Ginestra and P. Partono, Langmuir 5 (1989) 917.
[11] J. Jimenez-Jimenez, J. Merida-Robles, E. Rodriguez-Castellon, A. Jimenez-Lopez, M.L. Granados, S. del Val, I. Melian Cabrera and J.L.G. Fierro, Catal. Today 2004.
[12] B.N. Reddy, B.M. Reddy and M. Subramanyam, J. Chem. Soc. Faraday Trans. 87 (1991) 1649.
[13] J.N. Armor, Appl. Catal.: B 1 (1992) 221.
[14] J.P. Dunn, P.R. Koppula, H.G. Stenger and I.E. Wachs, Appl. Catal.: B 19 (1998) 103.
[15] H. Bosch and F. Janssen, Catal. Today 2 (1988) 39.
[16] J.N. Armor (ed.), in: *ACS Symposium Series*, Vol. 552 (Am. Chem. Society, Washington, DC, 1994).
[17] M. Amiridis, R. Duevel and I.E. Wachs, Appl. Catal.: B 23 (1999) 111.
[18] I.E. Wachs, Chem. Eng. Sci. 45 (1990) 5900.
[19] G. Busca, G. Centi, L. Marchetti and F. Trifiro, Langmuir 2 (1986) 568.
[20] K.V. Narayana, B. David Raju, S. Khaja Masthan, V. Venkat Rao, P. Kanta Rao and A. Martin, J. Mol. Catal. A: Chem 223 (2004) 321.
[21] E. Rombi, I. Ferino, R. Monaci, C. Picciau, V. Solinas and R. Buzzoni, Appl. Catal.: A 266 (2004) 73.
[22] Ch. Srilaxmi, N. Lingaiah, A. Hussain, P.S. Sai Prasad, K.V. Narayana, A. Martin and B. Lücke, Catal. Commun. 5 (2004) 199.
[23] S. del Val, M.L. Granados, J.L.G. Fierro, J.S. Gonzalez and A.J. Lopez, J. Catal. 188 (1999) 203.
[24] Ch. Srilakshmi, N. Lingaiah, P. Nagaraju , P.S. Sai Prasad, K.V. Narayana, A. Martin and B. Lücke, Communicated to Appl. Catal.
[25] P. Villabrille, P. Vazquez, M. Blanco and C. Caceres, J. Colloid Interface 251 (2002) 151.
[26] L.R. Pizzo, P.G. Vazquez, C.V. Caceres and C.V. Blanco, in: *Proceedings of the 17th Symposium Iberoam. Catal.*, Vol. 1, Porto, Portugal, July 200, p. 563.
[27] B. Samuneva, P. Tzvetkova, I. Gugov and V. Dimitrov, J. Mater Sci. Lett. 15 (1996) 2180.
[28] D. Ilieva, B. Jivov, G. Bogachev, C. Petrov, I. Penkov and Y. Dimitriev, J. NonCryst. Solids 283 (2001) 195.
[29] Y. Nakagawa, O. Ono, H. Miyata and Y. Hubokawa, J. Chem. Soc., Faraday Trans. 79 (1983) 2929.
[30] F. Benvenutti, C. Carlini, P. Patrono, A.M.R. Galletti, G. Sbrana, M.A. Massucci and P. Galli, Appl. Catal.: A 193 (2000) 147.
[31] J.F. Moulder, W.F. Stickle, P.E. Sobol and K.D. Bomben, in: *Handbook of XPS* (Perkin Elmer Corporation, Eden Prairie, MN, 1992).
[32] K.V.R. Chary, G. Kishan, Ch. Praveen kumar, G. Vidyasagar and J.W. Niemantsverdriet, Appl. Catal.: A 245 (2003) 303.
[33] K.V.R. Chary, G. Kishan, K. Ramesh, Ch. Praveen Kumar and G. Vidyasagar, Langmuir 16 (2000) 7692.
[34] P. Courtine and E. Bordes, Appl. Catal.: A 157 (1997) 45.
[35] K.V. Narayana, A. Venugopal, K.S. Rama Rao, V. Venkat Rao, S. Khaja Masthan and P. Kanta Rao, Appl. Catal.: A 167 (1998) 11.
[36] A. Martin and B. Lucke, Catal. Today 57 (2000) 61.
[37] L. Forni, Appl. Catal. 20 (1986) 219.